Talanta 82 (2010) 640–645

Contents lists available at ScienceDirect

Talanta

journal homepage: www.elsevier.com/locate/talanta

Direct determination of *trans*-resveratrol in human plasma by spectrofluorimetry and second-order standard addition

Cristina D. Bernardes[a], Ronei J. Poppi[b,c], Marcelo M. Sena[a,c,*]

[a] Unidade Universitária de Ciências Exatas e Tecnológicas, Universidade Estadual de Goiás, P.O. Box 459, 75000-000 Anápolis, GO, Brazil
[b] Institute of Chemistry, University of Campinas, 13084-971 Campinas, SP, Brazil
[c] Instituto Nacional de Ciência e Tecnologia de Bioanalítica, 13083-970 Campinas, SP, Brazil

ARTICLE INFO

Article history:
Received 3 March 2010
Received in revised form 10 May 2010
Accepted 10 May 2010
Available online 16 May 2010

Keywords:
PARAFAC
Trans-resveratrol
Second-order advantage
Chemometrics
Molecular fluorescence
Blood

ABSTRACT

Trans-resveratrol (RVT) is an antioxidant found in red grapes and their derivatives, which has been related to the reduction of cardiovascular diseases and cancer incidence.

This work developed a new spectrofluorimetric–chemometric method for the direct determination of RVT in human plasma. For each measurement, excitation–emission matrices were obtained from 280 to 360 nm (excitation) and from 380 to 550 nm (emission). The strategy adopted in this work combined data treatment with parallel factor analysis (PARAFAC), for extracting the pure analyte signal, using the standard addition method, which permits determinations in the presence of a strong matrix effect caused by plasma analyte–protein binding. Plasma samples were diluted 10 times and, for each, four standard additions of RVT were performed, in triplicate. A specific PARAFAC model was built for the three replicates of each sample, from three-way arrays formed by five measurements (initial sample plus four additions), 17 excitation wavelengths and 86 emission wavelengths. The best models were selected with four factors and accounted for more than 99.90% of the data variance. The loadings obtained were related to RVT and three interferences. The scores related to the analyte were used for linear regressions and all standard addition curves presented correlation coefficients equal or greater than 0.99. Good results were obtained in the concentration range from 0.10 to 5.00 $\mu g\,mL^{-1}$, with recoveries between 94.0 and 110.0%. The proposed method was also validated through the estimates of several figures of merit: sensitivity, analytical sensitivity, selectivity, precision, and limits of detection and quantitation.

1. Introduction

Trans-resveratrol (RVT), *trans*-3,4′,5-trihydroxystilbene, is a phytoalexin compound found mainly in red grapes and their derivatives. It is a powerful antioxidant synthesized mainly in the skin of grapes as a response to fungal attacks, infections, stress, injuries, or UV irradiation [1–3]. Smaller amounts of RVT are also found in the leaves, seed and core of the grapes. RVT is also extracted from *Polygonum cuspidatum*, a plant found in China and Japan, which is used in oriental folk medicine [4]. The major part of the studies about resveratrol has been focused on the *trans* isomer, since the physiological activity of the *cis* isomer is not well elucidated. The *trans* isomer is thermodynamically more stable, due to the steric repulsion present in the *cis* molecule, and can be isomerized when exposed to intense UV irradiation [5]. *Cis*-resveratrol has not been found in *Vitis vinifera* grapes, but it has been detected in wines produced with this grape [6], being formed during the fermentation step as a product of *trans* isomerization or decomposition of a resveratrol polymer [7].

RVT was first isolated from the roots of white hellebore in 1940 [2], but its presence in *V. vinifera* grapes was discovered only in 1976 [1]. RVT attracted little interest until 1992, when it was postulated to explain some of the cardioprotective effects of red wines [8]. These effects have been associated to the French paradox, since the French population suffers a lower incidence of coronary heart disease, despite having a diet rich in saturated fats [9]. In addition, it has been demonstrated that RVT prevents several diseases, such as cancer [10] and cerebral ischemic injury [11], and increases stress resistance and lifespan in vertebrates [12]. As a consequence of publicizing these studies in recent years, RVT is now sold as a food supplement in many countries.

RVT has been determined in human or rat plasma by high performance liquid chromatography (HPLC) [5,13–21]. The great majority of these methods has determined just the *trans* isomer, while only two papers have simultaneously determined both the isomers [15,19]. The scarcity of methods for determining *cis*-resveratrol

* Corresponding author. Present address: Department of Chemistry, ICEx, Universidade Federal de Minas Gerais, Av. Antônio Carlos 6627, Pampulha, 31270-901 Belo Horizonte, MG, Brazil. Tel.: +55 31 34096389; fax: +55 31 34095700.
E-mail address: marcsen@ufmg.br (M.M. Sena).

0039-9140/$ – see front matter © 2010 Elsevier B.V. All rights reserved.
doi:10.1016/j.talanta.2010.05.024

is due to factors such as its lesser importance and the inexistence of available standards. All the methods for determining RVT demand tedious preliminary steps of extraction, pre-concentration and/or proteins precipitation. Spectrofluorimetry could be a sensitive alternative for direct determination of RVT, since it presents natural fluorescence. Nevertheless, direct determination of RVT in plasma is not feasible due to the presence of fluorescent interferences that overlap its spectrum. Moreover, the quenching of the analyte signal caused by the interactions between RVT and proteins [22] leads to an individual and strong matrix effect that hinders an external calibration. In recent years, the combination of spectrofluorimetric data and three-way chemometric tools, mainly parallel factor analysis (PARAFAC) [23], has been a way to overcome these difficulties and develop direct methods for determining drugs in complex biological matrices. This combination has allowed simplification of the experimental procedure. Besides the mathematical removal of the signal contribution of interferences by employing three-way chemometric methods, the matrix effect is overcome with the use of the standard addition method. This strategy has recently been applied not only to the determination of drugs in plasma or urine, such as fluoroquinolone antibiotics [24], salicylate [25], propranolol [26], ciprofloxacin [27] and terazosin hydrochloride [28], but also in food analyses for determining sulphaguanidine residues in honey [29], aflatoxin B1 in wheat [30] and tetracycline in whey milk [31]. Therefore, the objective of this work was to develop a method for direct determination of RVT in human plasma by combining spectrofluorimetry and the above-mentioned chemometric strategy. The proposed method was validated through the estimation of figures of merit, such as sensitivity, analytical sensitivity, selectivity, precision and limits of detection and quantitation.

2. PARAFAC and second-order standard addition

2.1. Parallel factor analysis

PARAFAC [23] is a generalization of principal component analysis (PCA) to higher-order data, which presents a unique solution independent of rotation. A PARAFAC model of a three-way array is given by three loading matrices, **A**, **B** and **C**, with elements a_{if}, b_{jf} and c_{kf}, respectively ($f = 1$ to F factors/triads). The trilinear model is found to minimize the sum of squares of the residues, e_{ijk}, in the model, which is represented as follows:

$$x_{ijk} = \sum_{f=1}^{F} a_{if} b_{jf} c_{kf} + e_{ijk} \quad (1)$$

The choice of the correct number of factors is a key step when using PARAFAC. Since there is no absolute criterion for this choice, it is usually made based on the variance accounted for by the model, the chemical knowledge of the system and the core consistency diagnostic (CORCONDIA) [32].

2.2. Second-order standard addition

The standard addition method is recognized as an alternative for calibration in the presence of matrix effects. Its combination with PARAFAC or other second-order calibration methods has led to the second-order standard addition method (SOSAM) [33]. SOSAM has the advantage of allowing the recovery of pure spectra of each component of the system by applying a minimum number of constraints to the model. A more important aspect when using second-order calibration methods is the so-called second-order advantage, defined as the ability to perform a determination in the presence of unknown/unexpected interferences [34,35]. It becomes unnecessary to include the natural background in the calibration set. There are two modes of obtaining second-order advantage from higher-order information: (1) combining data from calibration and test sample before computing the regression coefficients and (2) estimating loadings from calibration data only, with the test sample leading to sample-specific regression coefficients in a subsequent step [35]. Among the methods of first mode, PARAFAC, direct trilinear decomposition (DTLD) [36], generalized rank annihilation method (GRAM) [37] and multivariate curve resolution-alternating least squares (MCR-ALS) [38] can be cited. In this work, the most popular PARAFAC was used. It presents the advantage of being more robust to data noise, what sometimes hinders the use of DTLD and GRAM in real noisy data. These two methods may also occasionally produce imaginary solutions and exhibit inflated variance [39]. Another advantage of PARAFAC over GRAM is that it allows multiple standard additions in SOSAM, as opposed to GRAM, which is limited to only one. A recent published alternative to cope with SOSAM when more than one interference occurs in the test samples is parallel profiles with linear dependencies (PARALIND) [40,41]. Examples of obtaining second-order advantage by the second mode are the combinations of residual bilinearization with bilinear least squares (BLLS/RBL) [42], unfold partial least squares (U-PLS/RBL) [43] and N-way PLS (RBL/N-PLS) [44]. A more complete discussion about the combination of PARAFAC and SOSAM can be found in other references [25,26,35,45].

2.3. Figures of merit

The estimation of figures of merit (FOM) is a key requisite for the validation of multivariate (first-order) and multidimensional (second-order) calibration methods, aiming at their future recognition by regulatory agencies and organisms. For univariate (zeroth-order) methods, the estimation of FOM is well known and established. For higher-order calibration methods, FOM such as sensitivity, selectivity and limit of detection are estimated based on the net analyte signal (NAS), which is defined as the part of the analytical signal that is related uniquely to the analyte of interest and is orthogonal to the signal of sample interferences [46]. For second-order methods, different ways of estimating NAS have been proposed in the literature [47–49]. A deeper discussion comparing these ways can be found elsewhere [50,51].

In this work, sensitivity (SEN) was estimated according to Eq. (2), which is the specific form of the general expression proposed by Olivieri and Faber [52], taking into account that only one analyte is determined. This is the most recent and suitable proposed expression for estimating SEN in second-order calibration models [51], which is used independent of the method employed for calculating NAS:

$$\mathrm{SEN} = g\{[(\boldsymbol{b}^T \boldsymbol{P}_{b,\ \mathrm{int}} \boldsymbol{b}) \times (\boldsymbol{c}^T \boldsymbol{P}_{c,\ \mathrm{int}} \boldsymbol{c})]^{-1}\}^{-1/2} \quad (2)$$

In Eq. (2), '*' indicates the element-wise Hadamard matrix product, **b** and **c** are the vectors containing the analyte profiles in the second and third dimensions, respectively; $\mathbf{P}_{b,\mathrm{int}}$ and $\mathbf{P}_{c,\mathrm{int}}$ are the projection matrices that remove the contribution from interferences in the second and third dimensions, respectively. All these matrices and vectors contain only normalized profiles. The scalar g is the integrated total signal for the analyte at unit concentration. When using PARAFAC, g corresponds to the slope of the straight line fitted between the scores of calibration samples and reference concentrations of the analyte. Selectivity (SEL) was also estimated according to Olivieri and Faber [52], as expressed in Eq. (3):

$$\mathrm{SEL} = \{[(\boldsymbol{b}^T \boldsymbol{P}_{b,\ \mathrm{int}} \boldsymbol{b}) \times (\boldsymbol{c}^T \boldsymbol{P}_{c,\ \mathrm{int}} \boldsymbol{c})]\}^{-1/2} \quad (3)$$

where the profiles of all the species are normalized. Analytical sensitivity (γ) was defined as the ratio between SEN and instrumental noise (ε), according to Eq. (4). The estimation of ε is calculated as the pooled standard deviation of the analyte signal in each wavelength

and it was obtained in this work from 10 blank replicates:

$$\gamma = \frac{\mathrm{SEN}}{\varepsilon} \quad (4)$$

The inverse of γ (γ^{-1}) establishes a minimum concentration difference that is discernible by the analytical method considering the experimental noise as the only source of error, regardless of the specific technique employed. The limits of detection (LOD) and quantitation (LOQ) were estimated according to Eqs. (5) and (6), respectively:

$$\mathrm{LOD} = 3.3\frac{\varepsilon}{\mathrm{SEN}} \quad (5)$$

$$\mathrm{LOQ} = 10\frac{\varepsilon}{\mathrm{SEN}} \quad (6)$$

Besides these FOM, accuracy, as the recovery for each concentration level, and precision, as its respective standard deviation (repeatability), were also estimated.

It is important to stress that when second-order standard addition is used, FOM such as SEN, SEL, γ, LOD and LOQ are sample-specific and cannot be defined for the method as a whole. In such cases, the authors sometimes report average values for a set of samples [26,39].

3. Experimental

3.1. Reagents, solutions and samples

RVT (98.3%) was kindly provided by Pharma Nostra (Anápolis, Brazil). A 100.0 μg mL^{-1} stock solution of RVT was prepared in ethanol (Synth, Brazil), since RVT has low solubility in water. From this, a dilute solution at 10.0 μg mL^{-1} in RVT was prepared in deionised water (Milli-Q). All the buffers used were prepared from a 0.1 mol L^{-1} universal buffer solution for UV spectrophotometric measurements composed of citric acid (Sigma), potassium monobasic phosphate (Synth), sodium tetraborate (Ecibra, Brazil), tris(hydroxymethyl)aminomethane (Sigma) and potassium chloride (Synth), with an appropriate amount of 0.4 mol L^{-1} HCl (Nuclear, Brazil) or 0.4 mol L^{-1} NaOH (Nuclear) [53]. Human plasma samples (fresh frozen plasma) of five healthy volunteers, who had diets without RVT for at least 1 week, where obtained at the Hemocentro of the University of Campinas and were kept in the freezer at −8 °C. It was assumed that the RVT concentration of the plasma samples is zero. All the glassware used was previously cleaned with 10% (v/v) HNO_3 (Synth) and then with deionised water.

3.2. Apparatus and software

The spectra were obtained in a Varian Cary Eclipse Spectrofluorimeter, using a 10.00 mm quartz cuvette. Measurements of pH were carried out in a Corning 350 pH meter. The data were imported using a homemade program and treated in MATLAB Version 6.5 (The MathWorks, Natick, USA). The PARAFAC calculations were carried out with the N-way toolbox for Matlab Version 2.10 [54]. A homemade routine was used for estimating SEN, SEL, γ, LOD and LOQ.

3.3. Procedure

A previous experiment was carried out aiming at estimating the distribution of acid and base forms of RVT as a function of pH. Twenty-one 3.00 μg mL^{-1} RVT solutions were prepared in deionised water and buffered in pH values from 5.0 to 9.6.

For RVT determination by standard addition, plasma samples were spiked with appropriate amounts of standard solutions, resulting in an RVT concentration range from 0.10 to 5.00 μg mL^{-1}. The plasma from a different individual was employed for each concentration level. All the samples were diluted 10 times in deionised water. Five 10.00 mL volumetric flasks were used for each measurement; in each flask, 1.00 mL of diluted RVT spiked plasma was added followed by 1.00 mL of a pH 5.00 buffer solution; then, 0, 50, 100, 150 and 200 μL of a 10.00 μg mL^{-1} RVT standard solution were added, respectively, to each of the five flasks. All the flasks were completed to the mark with deionised water. All the determinations were carried out in triplicate. Ten replicates of a blank sample (non-spiked diluted plasma) were also recorded for estimating instrument noise.

All the spectral surfaces were obtained in the excitation range from 280 to 360 nm (5 nm steps) and in the emission range from 380 to 550 nm (2 nm steps). The excitation and emission monochromator slit widths were 5.0 and 10.0 nm, respectively, and the scanning rate was 9600 nm min^{-1}.

4. Results and discussion

Some precautions were taken during the experiments in order to prevent RVT isomerization to the *cis* form, which presents lower fluorescence than the *trans* form [55]. All the working solutions were prepared fresh daily and protected with aluminum foil. A rapid scanning rate was chosen in order to reduce the exposure time of RVT to irradiation during the measurements. In a preliminary test, excitation–emission matrices (EEMs) of a 3.00 μg mL^{-1} RVT solution were obtained in triplicate and no perceptible change was noted in these spectra. Thus, it was concluded that the prevention of *cis* isomerization was assured. Another important variable was the pH of the measurements. It has been reported that RVT presents maximum emission intensity at pH 10 [56], but considering the estimated pK_a values found in the literature [56–59], the system should be more complex, since more than one RVT emission species might be present. Thus, an experiment was carried out aiming at estimating pK_{a1} of RVT.

4.1. Estimation of pK_{a1} of RVT through a PARAFAC model

A PARAFAC model can be used for estimating acid–base distribution profiles and pK_a values based on spectrophotometric data [60]. Thus, EEMs of 3.00 μg mL^{-1} RVT solutions in deionised water were obtained over the pH range from 5.0 to 9.6. An array formed by 21 pH values, 17 excitation wavelengths and 86 emission wavelengths was decomposed and the best PARAFAC model was selected with non-negativity constraints in all the modes and two factors, which were associated with acidic and basic RVT forms. The loadings related to excitation and emission spectra are shown in Fig. 1. Moreover, the loadings of the first mode provided a distribution profile of RVT forms (Fig. 2). Two third-order polynomial curves were fitted to acidic and basic distributions, and the intersection of these curves provides an estimation of the pK_{a1} of RVT of 8.7. This value is very close to 8.8, which was determined spectrofluorimetrically [56]. Other values found in the literature are 8.2 [57] and 8.3 [58], both determined by UV/vis absorbance spectrophotometry, and 9.49 [59], determined by capillary electrophoresis. It is important to note that spectrofluorimetrically estimated pK_a values correspond to excited molecular states that in most cases are different from values for the fundamental state. Considering these results and taking into account that RVT has a slower isomerization within a pH range from 5.0 to 8.0 [61], it was decided to conduct RVT determination in plasma buffered at pH 5.0.

4.2. RVT determination in plasma

Fig. 3 displays spectral surfaces of a pure plasma sample and the same sample spiked with 0.50 μg mL^{-1} of RVT. Pure plasma shows

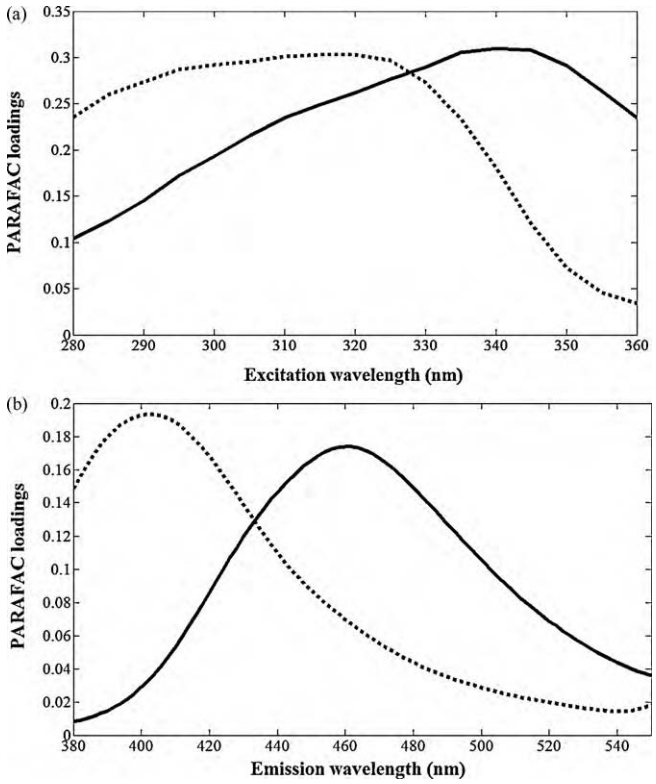

Fig. 1. Deconvoluted (a) excitation and (b) emission spectra of acidic (dotted line) and basic (solid line) forms of RVT in water obtained through the loadings of a PARAFAC model.

an intense band with excitation/emission maxima at 300/380 nm (Fig. 3a). After RVT addition, as a result of the sum of intensities of plasma and RVT, the observed band widened and increased (Fig. 3b). Nevertheless, this spectral change is somewhat difficult to be visualized, because the signal of RVT is strongly overlapped by tryptophan. Tryptophan presents a broad and intense fluorescence band centered at excitation/emission of 298/348 nm [62], being the main interference in this spectral region of human plasma. As can be seen in Fig. 1, RVT acidic form (the species determined here) in pure water presents excitation/emission maxima at 316/403 nm.

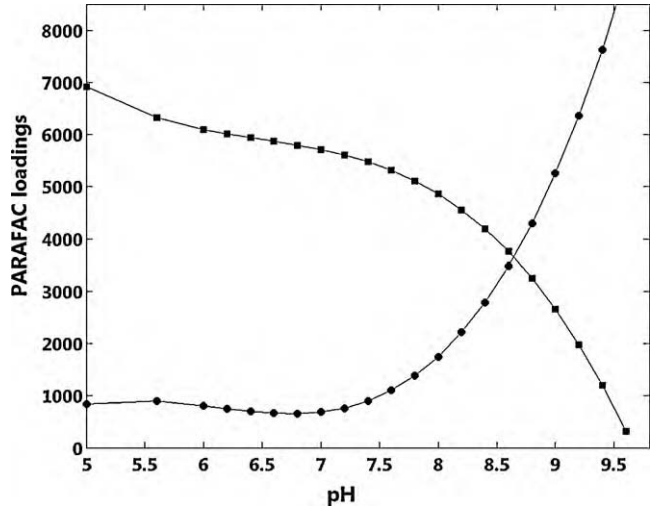

Fig. 2. Estimation of pK_{a1} of RVT. Distribution of acidic (squares) and basic (circles) forms of RVT in water as a function of the pH, obtained through the first dimension loadings of a PARAFAC model. The loadings were fitted to third-order polynomial curves.

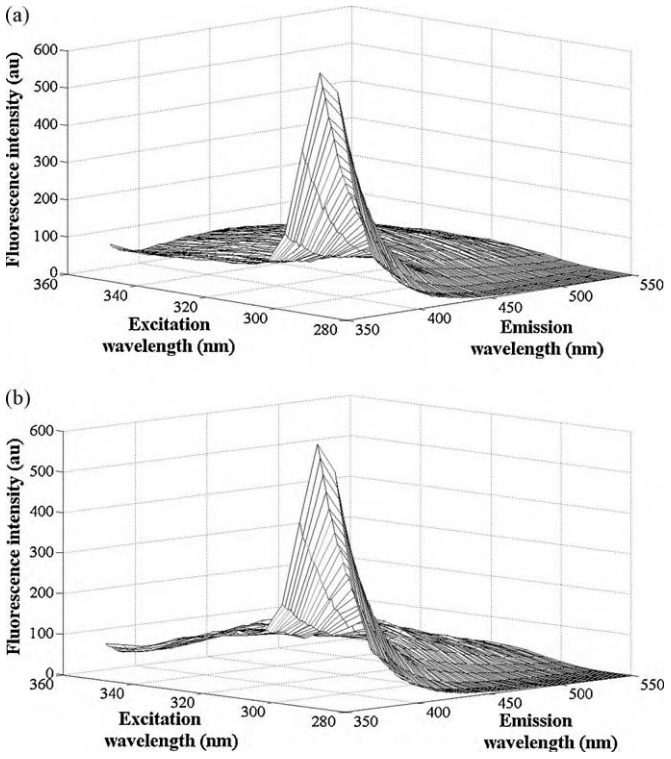

Fig. 3. Excitation–emission surfaces of (a) a pure plasma sample and (b) a sample of this same plasma spiked with 0.50 μg mL^{-1} RVT.

It is also important to mention that the initial part of the wavelength region corresponding to RVT emission was excluded from the analysis due to the presence of Rayleigh scatter, which shows no linear behavior and therefore cannot be modelled by PARAFAC. An attempt to alternatively use a missing values routine provided poor results.

The concentration range chosen for RVT determination was from 0.10 to 5.00 μg mL^{-1}, in accordance with the relevant literature [5,13–21]. As already mentioned, the interaction between RVT and serum proteins leads to a remarkable fluorescence quenching [22]. Three previous tests also demonstrated the presence of an individual matrix effect, since the RVT emission fluorescence was quenched in plasma to an extent that varied from sample to sample. Firstly, a spectral array formed by three different plasma samples spiked with the same RVT concentration (2.00 μg mL^{-1}) was decomposed by a PARAFAC model and the resulting scores (sample loadings) related to RVT showed more than 100% of difference. Secondly, an EEM for a plasma sample spiked with 2.0 μg mL^{-1} was digitally subtracted from an EEM for the same plasma sample not spiked with RVT. The resulting spectral surface was compared with a sample of 2.0 μg mL^{-1} of RVT in pure water, and the observed intensity maximum was about four times higher in water than in plasma. Finally, this matrix effect can also be observed in Fig. 4. Here, a plot of PARAFAC scores obtained for the five different plasmas used in this work, each one spiked with a different analyte concentration level, is shown. As can be seen, there is no linear relationship between these scores and the RVT concentration. These observations corroborated the impossibility of using an external calibration and led to the choice of standard addition. The chosen strategy uses PARAFAC scores, which are equivalent to the interference-free RVT signal, for plotting standard addition curves. The determinations were carried out in the classical situation of constant total volume.

A PARAFAC model was built for the three repetitions of each sample from arrays formed by five measurements (0–4 standard

Table 1
Results obtained for RVT determination in plasma.

Plasma sample	Expected RVT concentration ($\mu g\,mL^{-1}$)	Predicted RVT concentration ($\mu g\,mL^{-1}$)[a]	Recovery (%)	Number of factors	CORCONDIA (%)	Regression error ($\mu g\,mL^{-1}$)
1	0.10	0.11 ± 0.02	110.0	6	2	0.01
2	0.50	0.47 ± 0.06	94.0	4	12	−0.03
3	1.00	1.06 ± 0.06	106.0	4	52	0.06
4	2.00	1.91 ± 0.08	95.5	4	58	−0.09
5	5.00	5.37 ± 0.02	107.4	4	14	0.37

[a] Mean and standard deviation of three determinations.

additions), 17 excitation wavelengths and 86 emission wavelengths, totalising 15 models. Models with 2–8 factors were tested. The best models were selected with four factors in the most of the cases, non-negativity constraints on the tree modes and always accounted for more than 99.90% of total data variance. Table 1 shows the number of extracted factors and the respective CORCONDIA mean values for the best PARAFAC models. These values varied between 2 and 58%, pointing out that the models include both trilinear and non-trilinear variations. Nevertheless, the best models were chosen as a function of the lowest prediction errors, not of trilinearity consistence. Models with three factors presented almost 100% of trilinearity consistence, but much larger errors of prediction and residual variance. The factors obtained were related to RVT and three interferences. In one case, five interferences were modelled, meaning the presence of two more fluorescent species in the composition of this specific plasma sample. The scores and loadings obtained are shown in Fig. 5. PARAFAC loadings (Fig. 5b and c) allowed identification of interference 1 as tryptophan and suggested nicotinamide adenine dinucleotide (NADH) and riboflavin or their metabolites as possibilities for attribution to interferences 2 and 3 [62]. The scores plot (Fig. 5a) shows that only RVT scores change with standard additions while the remaining components (interferences) stay almost constant. RVT scores were used in univariate linear regressions and all the standard addition curves presented correlation coefficients (r) of at least 0.99. Table 1 also shows the predictions, the percentage of recovery and the regression errors for each sample. The recovery varied from 94.0 to 110.0%. At a 95% confidence level t-tests showed that there are no significant differences between the predicted and reference concentration values for the first four plasma samples.

4.3. Estimation of figures of merit

Table 2 shows the estimations for SEN, SEL, γ, LOD and LOQ. As previously discussed (Section 2.3), in the present situation these FOM are sample-specific. Since there are great differences among the plasma samples, it was considered not representative to express FOM for the method as a whole. These great differences demonstrated the strong individual matrix effect that leads to different levels of fluorescence quenching. It is very interesting to note the consistency between the results of Table 2 and Fig. 4. The lower the score sample in Fig. 4, meaning high levels of quenching, the lower the SEN for determination of this sample.

The values of γ^{-1} provided good estimations of concentration differences that the method is able to discern in the absence of experimental error. LOD and LOQ estimated values are considered

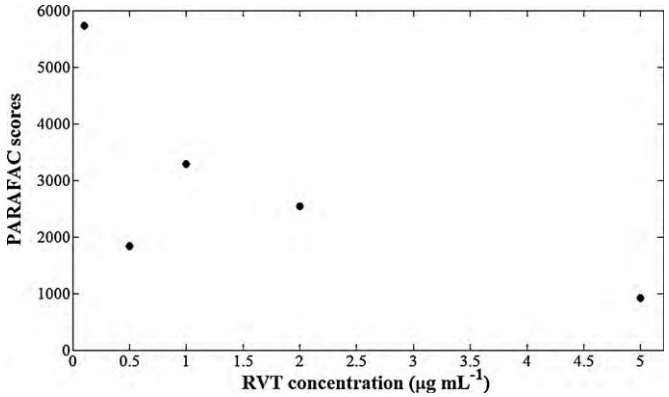

Fig. 4. Scores obtained for a PARAFAC model for five different plasma samples, each one spiked with a different RVT concentration level.

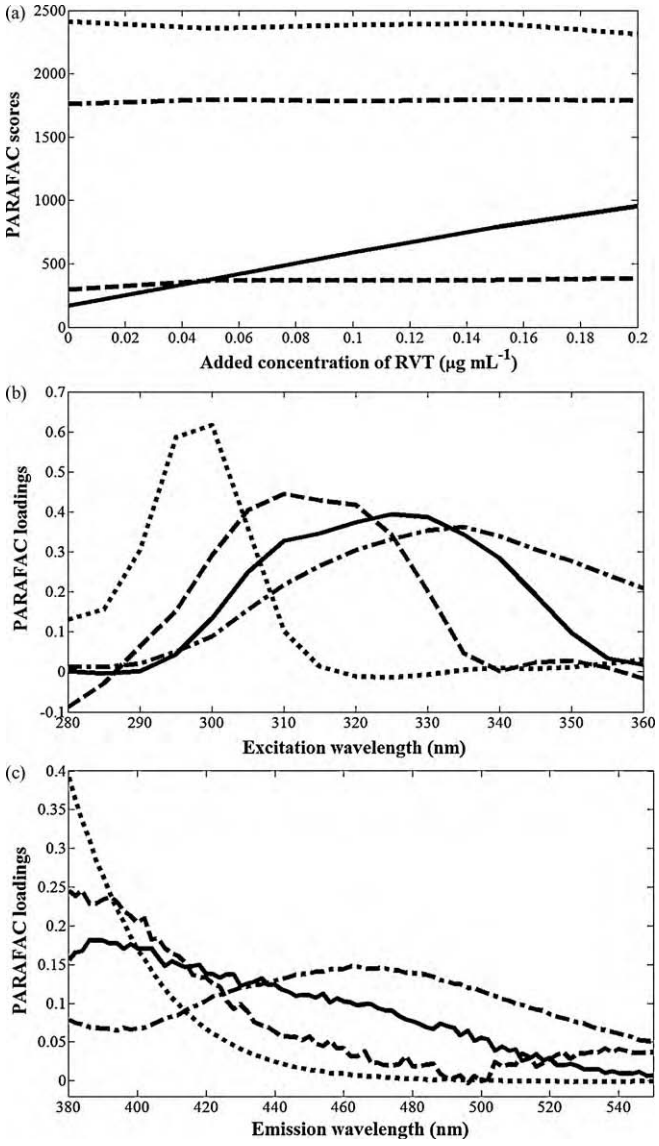

Fig. 5. PARAFAC-SOSAM model for RVT determination in plasma. (a) Scores; (b) excitation loadings; (c) emission loadings. Solid line: RVT; dotted line: tryptophan; dashed line: interference 2; dash-dotted line: interference 3.

Table 2
Estimated figures of merit.

Plasma sample	RVT concentration ($\mu g\,mL^{-1}$)	SEN[a]	SEL	γ ($mL\,\mu g^{-1}$)	γ^{-1} ($\mu g\,mL^{-1}$)	LOD ($\mu g\,mL^{-1}$)	LOQ ($\mu g\,mL^{-1}$)
1	0.10	1450	0.15	1.9×10^3	0.001	0.002	0.005
2	0.50	316	0.08	4.1×10^2	0.002	0.008	0.024
3	1.00	1050	0.08	1.4×10^3	0.002	0.002	0.007
4	2.00	632	0.11	8.2×10^2	0.003	0.004	0.012
5	5.00	182	0.05	2.4×10^3	0.011	0.013	0.042

[a] Values expressed as the ratios between the units of fluorescence intensity and of concentration ($\mu g\,mL^{-1}$).

suitable for clinical analysis. Besides these FOM, accuracy was also evaluated, through a mean recovery of 102.6%, and precision, at the level of repeatability, providing a mean standard deviation of 8.1% (Table 1).

5. Conclusions

In recent years, RVT has become an analyte of increasing interest, due its antioxidant properties and its association with the French paradox. This work developed a method for direct determination of RVT in human plasma. The analytical strategy employed combined spectrofluorimetric data and the second-order advantage for determination in the presence of uncalibrated interferences without need of prior extraction or separation steps. Good results were obtained in the concentration range from 0.10 to 5.00 $\mu g\,mL^{-1}$ with errors of prediction of at maximum 10%. The method was also validated by using the most recent proposed expressions for estimating FOM for second-order methods. Among the advantages of this method over the traditional HPLC procedures, low cost, speed, lack of need for reagents or solvents and no production of chemical waste can be cited. The acquisition of one spectral surface requires less than 1 min, which can be compared with the time spent for a typical chromatographic run for RVT determination, which was 11 min [5]. The contribution of this work could be extended to developing methods for the determination of RVT in other complex matrices, such as wines and grape juices.

Acknowledgements

The authors thank the HEMOCENTRO of UNICAMP and the volunteers, who provided the plasma samples, Pharma Nostra for RVT standard, Dr. Jez W.B. Braga (IQ-UnB, Brasília) for valuable discussions about FOM for second-order methods, and Prof. Carol H. Collins (IQ-UNICAMP, Campinas) for English revision. C.D.B. thanks CAPES (PROCAD 1516/2007) for a fellowship.

References

[1] P. Langcake, R.J. Pryce, Physiol. Plant Pathol. 9 (1976) 77.
[2] J.A. Baur, D.A. Sinclair, Nat. Rev. Drug Discov. 5 (2006) 493.
[3] E. Cantos, J.C. Espin, M.J. Fernandez, J. Oliva, F.A. Tomas-Barberan, J. Agric. Food Chem. 51 (2003) 1208.
[4] H. Arichi, Y. Kimura, H. Okuda, K. Baba, M. Kozawa, S. Arichi, Chem. Pharm. Bull. 30 (1982) 1766.
[5] A. Katsagonis, J. Atta-Politou, M.A. Koupparis, J. Liq. Chromatogr. Relat. Technol. 28 (2005) 1393.
[6] D.M. Goldberg, E. Ng, A. Karumanchiri, J. Yan, E.P. Diamandis, G.J. Soleas, J. Chromatogr. A 708 (1995) 89.
[7] J.P. Roggero, Sci. Aliments 16 (1996) 631.
[8] E.H. Siemann, L.L. Creasy, Am. J. Enol. Viticult. 43 (1992) 49.
[9] S. Renaud, M. Lorgeril, Lancet 339 (1992) 1523.
[10] M. Jang, L. Cai, G.O. Udeani, K.V. Slowing, C.F. Thomas, C.W.W. Beecher, H.H.S. Fong, N.R. Farnsworth, A.D. Kinghorn, R.G. Mehta, R.C. Moon, J.M. Pezzuto, Science 275 (1997) 218.
[11] Q. Wang, J. Xu, G.E. Rottinghaus, A. Simonyi, D. Lubahn, G.Y. Sun, A.Y. Sun, Brain Res. 958 (2002) 439.
[12] D.R. Valenzano, E. Terzibasi, T. Genade, A. Cattaneo, L. Domenici, A. Cellerino, Curr. Biol. 16 (2006) 296.
[13] Z. Zhu, G. Klironomos, A. Vachereau, L. Neirinck, D.W. Goodman, J. Chromatogr. B 724 (1999) 389.
[14] M.E. Juan, R.M. Lamuela-Raventos, M.C. Torre-Boronat, J.M. Planas, Anal. Chem. 71 (1999) 747.
[15] C. Giachetti, C. Tognolo, P. Gnemi, A. Tenconi, Chromatographia 50 (1999) 571.
[16] Y. Zhu, T. Huang, M. Cregor, H. Long, C.B. Kissinger, P.T. Kissinger, J. Chromatogr. B 740 (2000) 129.
[17] M.E. Juan, J. Buenafuente, I. Casals, J.M. Planas, Food Res. Int. 35 (2002) 195.
[18] H. He, X. Chen, G. Wang, J. Wang, A.K. Davey, J. Chromatogr. B 832 (2006) 177.
[19] X. Chen, H. He, G. Wang, B. Yang, W. Ren, L. Ma, Q. Yu, Biomed. Chromatogr. 21 (2007) 257.
[20] H. He, X.J. Chen, G.J. Wang, Chromatographia 68 (2008) 1013.
[21] M.E. Juan, M. Maijó, J.M. Planas, J. Pharm. Biomed. Anal. 51 (2010) 351.
[22] S. Cao, D. Wang, X. Tan, J. Chen, J. Sol. Chem. 38 (2009) 1193.
[23] R. Bro, Chemom. Intell. Lab. Syst. 38 (1997) 149.
[24] A. Muñoz de la Peña, A. Espinosa Mansilla, D. González Gómez, A.C. Olivieri, H.C. Goicoechea, Anal. Chem. 75 (2003) 2640.
[25] M.M. Sena, M.G. Trevisan, R.J. Poppi, Talanta 68 (2006) 1707.
[26] L.C. Silva, M.G. Trevisan, R.J. Poppi, M.M. Sena, Anal. Chim. Acta 595 (2007) 282.
[27] M.C. Ortiz, L.A. Sarabia, M.S. Sanchez, D. Gimenez, Anal. Chim. Acta 642 (2009) 193.
[28] H.Y. Zou, H.L. Wu, L.Q. Ouyang, Y. Zhang, J.F. Nie, H.Y. Fu, R.Q. Yu, Anal. Chim. Acta 650 (2009) 143.
[29] A. Muñoz de la Peña, N. Mora Diez, M.C. Mahedero García, D. Bohoyo Gil, F. Cañada-Cañada, Talanta 73 (2007) 304.
[30] J. Hashemi, G.A. Kram, N. Alizadeh, Talanta 75 (2008) 1075.
[31] N. Rodríguez, B.D. Real, M.C. Ortiz, L.A. Sarabia, A. Herrero, Anal. Chim. Acta 632 (2009) 42.
[32] R. Bro, H.A.L. Kiers, J. Chemom. 17 (2003) 274.
[33] K. Booksh, J.M. Henshaw, L.W. Burgess, B.R. Kowalski, J. Chemom. 9 (1995) 263.
[34] K.S. Booksh, B.R. Kowalski, Anal. Chem. 66 (1994) 782A.
[35] G.M. Escandar, N.M. Faber, H.C. Goicoechea, A. Muñoz de La Peña, A.C. Olivieri, R.J. Poppi, Trends Anal. Chem. 26 (2007) 752.
[36] E. Sanchez, B.R. Kowalski, J. Chemom. 4 (1990) 29.
[37] E. Sanchez, B.R. Kowalski, Anal. Chem. 58 (1986) 496.
[38] R. Tauler, Chemom. Intell. Lab. Syst. 30 (1995) 133.
[39] A.L. Xia, H.L. Wu, D.M. Fang, Y.J. Ding, L.Q. Hu, R.Q. Yu, Anal. Sci. 22 (2006) 1189.
[40] M. Bahram, R. Bro, Anal. Chim. Acta 584 (2007) 397.
[41] R. Bro, R.A. Harshman, N.D. Sidiropoulos, M.E. Lundy, J. Chemom. 23 (2009) 324.
[42] P.C. Damiani, A.J. Nepote, M. Bearzotti, A.C. Olivieri, Anal. Chem. 76 (2004) 2798.
[43] A.C. Olivieri, J. Chemom. 19 (2005) 253.
[44] V.A. Lozano, G.A. Ibañez, A.C. Olivieri, Anal. Chim. Acta 615 (2009) 165.
[45] M.M. Sena, M.G. Trevisan, R.J. Poppi, Quim. Nova 28 (2005) 910.
[46] A. Lorber, Anal. Chem. 58 (1986) 1167.
[47] C.N. Ho, G.D. Christian, E.R. Davidson, Anal. Chem. 52 (1980) 1071.
[48] Y. Wang, O.S. Borgen, B.R. Kowalski, J. Chemom. 7 (1993) 117.
[49] N.J. Messick, J.H. Kalivas, P.M. Lang, Anal. Chem. 68 (1996) 1572.
[50] A.C. Olivieri, Anal. Chem. 77 (2005) 4946.
[51] P. Valderrama, J.W.B. Braga, R.J. Poppi, Quim. Nova 32 (2009) 1278.
[52] A.C. Olivieri, N.M. Faber, J. Chemom. 19 (2005) 583.
[53] D.D. Perrin, B. Dempsey, Buffers for pH and Metal Ion Control, Chapman and Hall, New York, 1974.
[54] C.A. Andersson, R. Bro, Chemom. Intell. Lab. Syst. 52 (2000) 1.
[55] L. Camont, C.H. Cottart, Y. Rhayem, V. Nivet-Antoine, R. Djelidi, F. Collin, J.L. Beaudeux, D. Bonnefont-Rousselot, Anal. Chim. Acta 634 (2009) 121.
[56] J.M. López-Nicolás, F. García-Carmona, J. Agric. Food Chem. 56 (2008) 7600.
[57] T. Galeano Díaz, I. Durán Merás, D. Airado Rodríguez, Anal. Bioanal. Chem. 387 (2007) 1999.
[58] Y. Takagai, T. Kubota, H. Kobayashi, T. Tashiro, A. Takahashi, S. Igarashi, Anal. Sci. 21 (2005) 183.
[59] J. Cao, G.H. Chen, Y.S. Du, F.F. Hou, Y.L. Tian, J. Liq. Chromatogr. Relat. Technol. 29 (2006) 1457.
[60] M.M. Sena, J.C.B. Fernandes, L. Rover Jr., R.J. Poppi, L.T. Kubota, Anal. Chim. Acta 409 (2000) 159.
[61] K.E. Allan, C.E. Lenehan, A.V. Ellis, Aust. J. Chem. 62 (2009) 921.
[62] O.S. Wolfbeis, M. Leiner, Anal. Chim. Acta 167 (1985) 203.